Design of diaphragm actuator based on ferromagnetic shape memory alloy composite

Yuanchang Liang[a], M. Taya[a], Yasuo Kuga[b]
[a]Center for Intelligent Materials and Systems, Department of Mechanical Engineering, University of Washington, Seattle, WA 98195-2600, USA
[b]Department of Electrical Engineering, University of Washington, Seattle, WA 98195-2500, USA

ABSTRACT

A new diaphragm actuator based on the ferromagnetic shape memory alloy (FSMA) composite is designed where the FSMA composite is composed of ferromagnetic soft iron and superelastic grade of NiTi shape memory alloy (SMA). The actuation mechanism for the FSMA composite plate of the actuator is the hybrid mechanism that we proposed previously. This diaphragm actuator is the first design toward designing a new synthetic jet actuator that will be used for active flow control technology on airplane wings. The design of the FSMA composite diaphragm actuator was established first by using both mechanical and ferromagnetic finite element analyses with an aim of optimization of the actuator components. Based on the FEM results, the first generation diaphragm actuator system was assembled and its static and dynamic performance was experimentally evaluated.

Keywords: shape memory alloy, active flow control, ferromagnetic, synthetic jet, superelasticity, martensitic transformation, hybrid mechanism, composite.

1. INTRODUCTION

It has been shown that active flow control technology can help aircraft improve aerodynamic performance, such as jet noise reduction and aerodynamic stall improvement by adding external energy into the flow field [1-7]. The active flow control can be achieved by injecting synthetic jets with high momentum air into the flow at the appropriate locations on aircraft wings. For example, the Boeing company has applied active flow control technology to rotorcraft, V22, focusing on alleviating rotor download on tiltrotor aircraft, for increasing the V22 mission capability on both payload and range [7]. Currently, most of the synthetic jet actuators have been constructed based on piezoelectric materials as actuator materials to produce synthetic jet flow [5-7]. However, piezoelectric materials may not produce large force to induce strong jet flow. Therefore, we are seeking another design approach of a synthetic jet actuator with a vibrating surface based on ferromagnetic shape memory alloy composite and the hybrid mechanism.

The strong attentions have been paid to ferromagnetic shape memory alloys (FSMAs) as actuator materials which are considered for fast responsive and high power, yet light weight actuators [8-10]. However, FSMAs driven by uniformly applied magnetic field has been found to produce small force. It is disadvantageous to use uniform (constant) magnetic field alone as a driving force [11-13]. Therefore, we proposed the hybrid mechanism that is adopted in the present paper for actuator applications [13-15]. The hybrid mechanism is based on the stress-induced martensitic phase transformation produced by applied magnetic field gradient, thus enhancing the displacement, as the stiffness of shape memory alloy reduces due to the martensitic phase transformation. We have designed the diaphragm actuator based on the composite material made of superelastic grade of NiTi shape memory alloy and ferromagnetic soft iron as a composite diaphragm driven by a hybrid magnet system [16]. This paper will present the finite element analysis of the diaphragm actuator (including the diaphragm and the hybrid magnet system) as well as experimental results of static and dynamic testing. The goal of the diaphragm actuator is to produce large force and reasonable stroke, hence, can be applied to active flow control technology.

2. ESTIMATION OF THE ACTUATOR SYSTEM

The diaphragm actuator system mainly consists of two composite diaphragms and a hybrid magnet system as shown in Figure 1(a). The composite diaphragm is composed of a superelastic grade NiTi SMA thin plate and a soft magnet pad. Two diaphragms simultaneously driven by the hybrid magnet system will vibrate (white arrows) and create a jet flow (black arrow), as shown in Figure 1(b). The hybrid magnet system and the superelastic property of the NiTi plate will ensure the reversible and large deformation at a reasonable fast actuation speed. The dimension of the first generation actuator is about 100mm in diameter and 50mm in height with only one composite diaphragm.

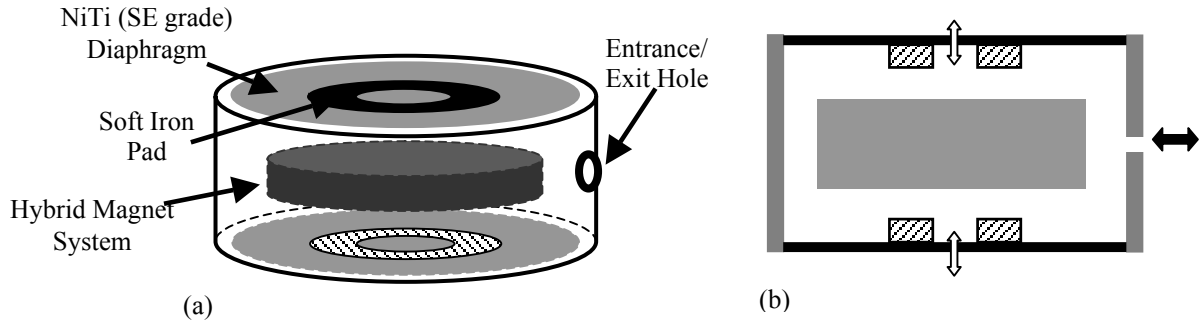

Figure 1 (a) The schematic of the diaphragm actuator system, (b) the jet flow (as shown by the black arrow) will be created by the vibration of the diaphragm (as shown by white arrows).

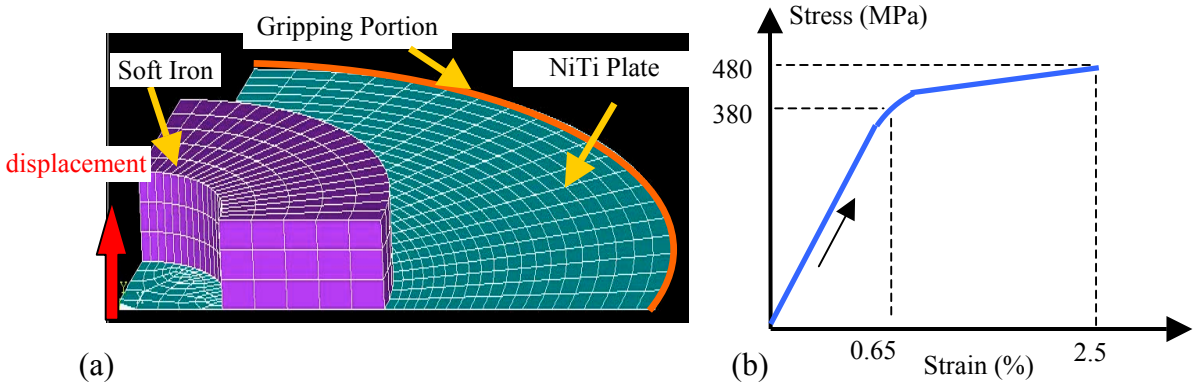

Figure 2 (a) ANSYS model of the quarter composite diaphragm, (b) the nonlinear stress-strain curve of NiTi SMA as input material data.

2.1 Mechanical FEM analysis of the composite diaphragm deformation

The deformation of the FSMA composite diaphragm is first estimated by ANSYS finite element static analysis. The FEM model has been established as a quarter of the composite diaphragm because of its axisymmetric geometry as shown in Figure 2(a). A nonlinear stress-strain curve of NiTi alloy provided by the vendor was used for the estimation, as shown in Figure 2(b). In this case, we use 480MPa as our limited design stress level to ensure the superelasticity of the NiTi plate. Due to the limitation of the FEM program, only the loading curve is used. The dimension of the NiTi plate is 90mm in diameter and 0.4mm in thickness. The soft magnet pad is made of iron with 4mm in thickness, 50mm in outer diameter and 25mm in inner diameter. The determination of the outer diameter of the soft magnet pad is based on the classic elasticity [17] and has to make compromise with the structure of the hybrid magnet system. It has been shown that if the ratio of the diameter of the plate to that of the distributed loading is about 2, during loading, the stress level on gripping portion will be the same as that on the area of NiTi plate connected with soft magnet pad. This

suggests that when an external load is applied on the pad, both gripping and connecting areas will simultaneously reach the stress level high enough to induced the martensitic phase transformation. Therefore, the composite diaphragm can exhibit larger deformation.

The predicted result of the force-displacement relationship at the center of the diaphragm is shown in Figure 3. Note that due to the rigid iron pad, the displacement of the composite diaphragm displacement within the area connected with the iron pad is uniform. This is an advantage to produce large volume of airflow for the synthetic jet application. Figure 3 clearly shows that the diaphragm is merely under the elastic deformation when the displacement is below 2mm. However, when the displacement reaches 2mm, the martensitic transformation occurs at the highest stress field areas on the diaphragm, i.e. near gripping portion and the area connected with the iron pad. Therefore, more deformation can be obtained due to the stress-induced martensitic phase transformation which makes NiTi material softer. Finally, the FEM simulation also shows that when the displacement reaches 5.6mm, the highest stress level does not yet reach 480MPa. Therefore, this will ensure the diaphragm without permanent deformation and it should return to original position upon unloading.

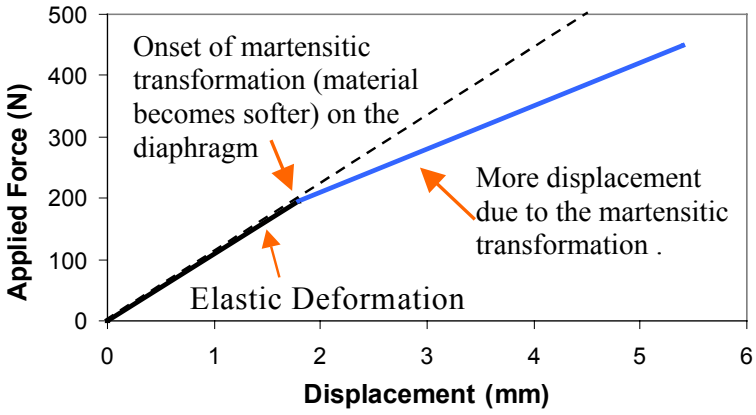

Figure 3 Estimated force-displacement of NiTi/soft iron diaphragm

2.2 Electromagnetic FEM analysis of the hybrid magnet system

The FSMA composite diaphragm will be driven by a magnet system based on the concept of the hybrid magnet [16]. The system basically consists of permanent magnet, yoke and solenoid wire. It has been shown that the hybrid magnet system is more efficient and produces much larger force than the traditional solenoid magnet [13-16]. For the present case of the diaphragm actuator, we can modify the first generation system from one-side diaphragm to the system with both side diaphragms without decreasing its performance, so two diaphragms can be driven for generating synthetic jet from the diaphragm actuator. To this end we performed electromagnetic FEM analysis on the magnetic flux and generate the force distributions by establishing a 2-D model as shown in Figure 4. The model is only the right half portion of the system due to its axisymmetric geometry. Both permanent magnets are ring shape with 44mm in outer diameter, 32mm in inner diameter and 4mm in thickness. They are polarized along their radius direction and made of Neodium (with Hc of 840 KA/m). Note that the polarized direction of the upper permanent magnet should be opposite to that of the bottom one, in order to establish an appropriated magnetic flux circuit. As shown in Figure 4(a), when the power is off, most of magnetic flux (clockwise) produced by both permanent magnets flows inside the yoke. Therefore, no force is available on soft iron pads. When the power is on, Figure 4(b), an opposite direction (counter clockwise) of magnetic flux is produced by input current. This new magnetic flux will force magnetic flux flowing out of the yoke around permanent magnets and produce a magnetic gradient. Therefore, the flux will go through soft iron pads and induce large force on both pads towards the magnet system.

By changing the distance between the soft iron pad and the hybrid magnet, a force-displacement curve of a pad can be generated. This means that the external force acting on the NiTi diaphragm produced by the magnet system is estimated

for a given position of the soft iron pad. Therefore, both estimated results of the composite diaphragm (Figure 3) and the force provided by the hybrid magnet system can be combined together as the static deformation of the diaphragm actuator, as shown in Figure 5. The dimension of the soft iron pad is about 50mm in outer diameter, 25mm in inner diameter and 6mm in thickness. The solid lines with symbols in Figure 5 are the force available to the diaphragm with respect to different levels of input current and the broken line is the force needed to deform the composite diaphragm. If we just input a current of 2 Amp, the diaphragm will exhibit 1.3mm since the broken line crosses the solid line at 1.3mm, i.e. the force induced from the magnet system is not enough to further deform the diaphragm. The estimated results show that an input current of 3 Amp can produce a displacement of 4mm on the diaphragm. When the displacement reaches 2mm, the martensitic transformation occurs on the diaphragm and less current is needed to produce more displacement.

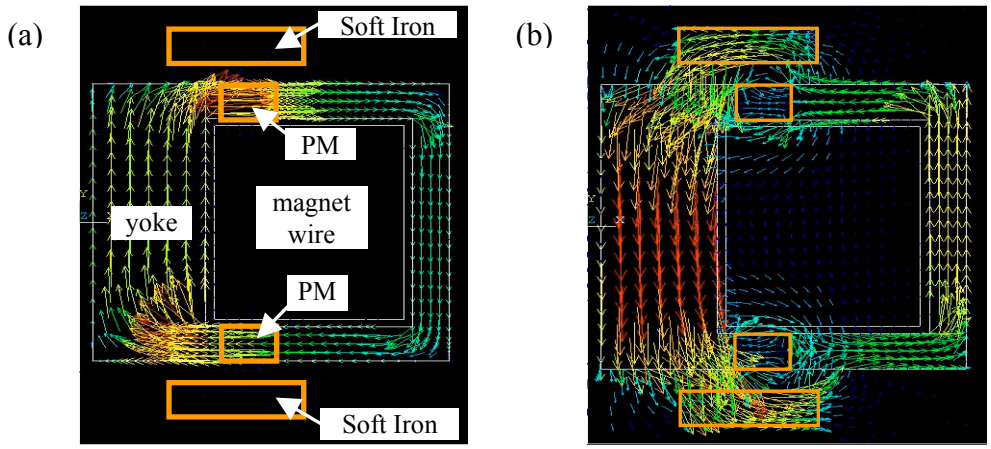

Figure 4 Electromagnetic FEM analysis simulates the function of the hybrid magnet system, (a) magnetic flux is flowing inside the yoke and no force is available on soft iron when the power is off, (b) magnetic flux go through soft iron pad and force is induced when the power is on

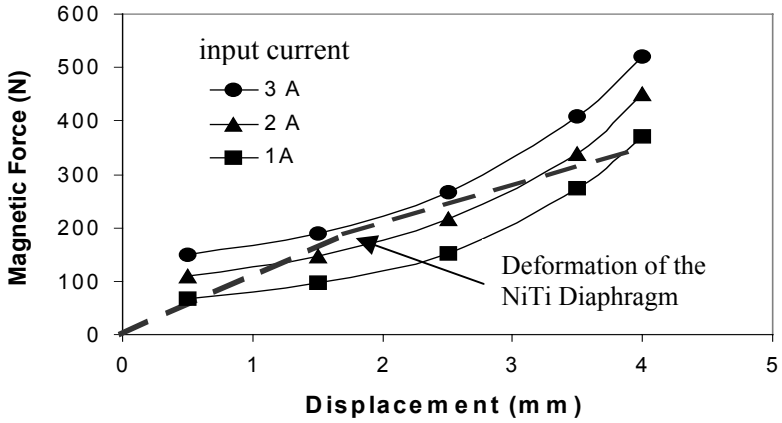

Figure 5 Estimated force-displacement relation of the diaphragm actuator

3. PERFORMANCE OF THE ACTUATOR SYSTEM WITH ONE-SIDE DIAPHRAGM

3.1 Testing system and components of the actuator

The testing system is shown schematically in Figure 6(a), including a function generator, an audio amplifier and a laser displacement measurement system. The laser displacement measurement system can control the laser measurement along the diameter of the diaphragm so the profile of the diaphragm is detected. The single step signal can be used for static performance test and a waveform signal for dynamic performance test. The FSMA composite diaphragm is also shown in Figure 6(b). The NiTi plate is about 0.4mm in thickness and 100mm in diameter. The soft iron pad is using the same size as described in the FEM simulation results shown in Figure 5 in Section 2.2. The connection between the NiTi plate and the soft iron pad is made by several screws with reinforcement of an aluminum ring on the opposite side of the plate. The pad and the yoke are made of low carbon steel.

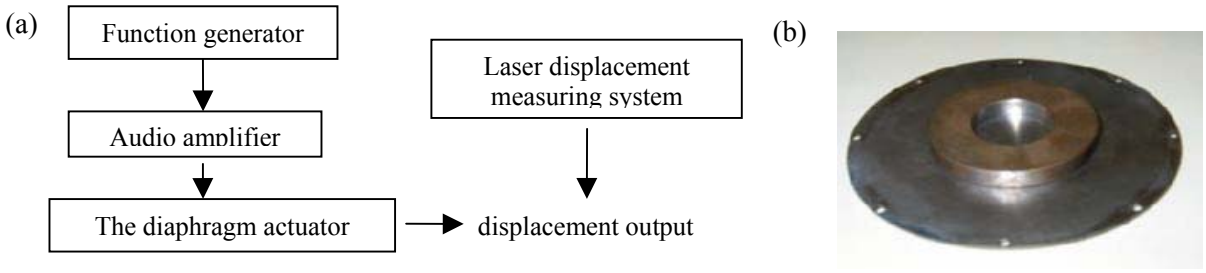

Figure 6 (a) Block diagram of measurement system for testing the performance of the diaphragm actuator, (b) the FSMA composite diaphragm

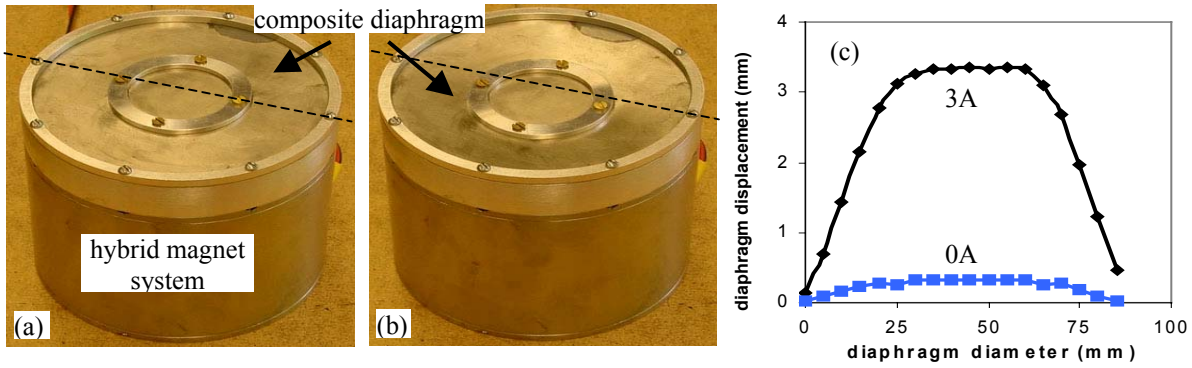

Figure 7 The photos of the diaphragm actuator, (a) power is off, (b) the diaphragm deforms downward when the power is on and (c) The cross section profile along the diameter of the diaphragm without input current (blue line) and with 3Amp current (black line).

3.2 Static performance test of the actuator

The static test of the diaphragm actuator is performed. The maximum input current is about 3 Amp for the system. The final assembly of the diaphragm system is shown in Figure 7(a) where the FSMA composite diaphragm is fixed on the top of the hybrid magnet system by screws and alumna rings. Figure 7(b) shows the photo of the diaphragm actuator after the actuation. The broken line is the original centerline of the diaphragm before the actuation as shown in Figure 7(a). The composite diaphragm clearly exhibits the downward deformation under a input current of 3 Amp. The profile across the diameter of the diaphragm was also detected by the laser measurement system as shown in Figure 7(c), where the symbols of filled and hollowed squares present with and without input current, respectively. The composite diaphragm has a 3mm displacement when the hybrid magnet is on. This result is close to the prediction by FEM

analysis as described in the previous sections. Furthermore, the martenstic phase transformation is induced when the displacement reaches 2mm. When the power is off, the diaphragm will spring back due to the superelasticity of NiTi shape memory alloy plate. If a larger current input is available, larger force can be obtained and more deformation of the diaphragm will occur.

3.3 Dynamic performance test of the actuator

The dynamic performance on the diaphragm actuator was tested as well. Figure 8(a) shows the input signal from the function generator and the audio amplifier. It is a 6Hz frequency and about 40V (peak to peak) sine waveform signal. The displacement response of the actuator is detected by the laser measuring system as shown in Figure 8(b). The diaphragm exhibited about 1.3mm displacement during the dynamic test. Figure 8 clearly shows that when the input signal is in a negative voltage (current), the actuator exhibits a very small displacement. This phenomenon can be explained by Figure 4 that the hybrid magnet system is used only at an opposite direction of the magnetic flux to the direction of the one produced by permanent magnet, as shown in Figure 4(b). Therefore, only positive input voltage (current) can effectively drive the actuator system. To improve the frequency response of the diaphragm actuator, it is necessary to decrease dimensions of the diaphragm and the soft iron pad. Also, the input signal of the power supply system has to be modified to satisfy the hybrid magnet system, i.e. only producing positive input voltage (current). This could improve the frequency response of the diaphragm actuator system.

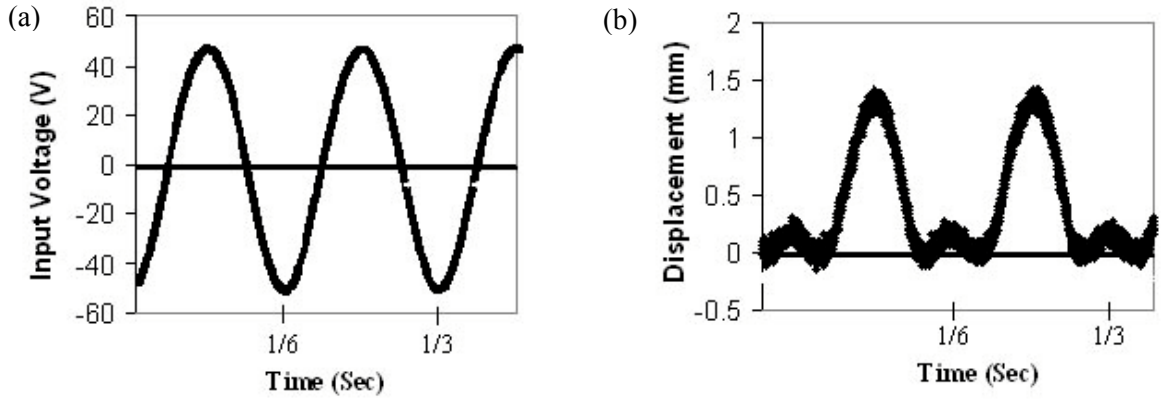

Figure 8 Results of the dynamic testing on the diaphragm actuator (a) input signal and (b) the actuator dynamic performance

4. CONCLUSION

The first generation of the diaphragm actuator made of ferromagnetic shape memory alloy (FSMA) composite, i.e. NiTi/soft iron, was designed by both mechanical and ferromagnetic finite element analyses, followed by the assembly of the actuator with one-side FSMA composite diaphragm. Then the static performance of the actuator was measured experimentally, in a good agreement with FEM analysis. Preliminary testing of the actuator under dynamic loading was also performed. It is expected that a new synthetic jet actuator can be designed based on the first generation actuator composed of FSMA composite.

ACKNOWLEDGEMENTS

This study was supported by DARPA-ONR contract (N-00014-00-1-0520). Dr. Roshdy Barsoum of ONR and Dr. John Main of DARPA are the program monitors. The present authors are thankful to Hitachi Metals (Mr. Masuzawa) for their assistance in providing ring-shaped permanent magnets, and also Mr. Suga of Nippon Cross Atueu and Mr. Kise of Kantoc in providing the superelastic NiTi plates.

REFERENCE

1. L. Pack and R. Joslin, "Overview of Active flow control at NASA Langley Research Center", *Proceedings of SPIE*, **3326**, pp. 202-213, 1999.
2. A. Honohan, M. Amitay and A. Glezer, "Aerodynamic Control Using Synthetic Jet", *AIAA Fluids*, June 2000, AIAA 2000-2401, 2000.
3. M. Amitay, A. Honohan, M. Trautman, and A. Glezer, "Modification of the Aerodynamic Characteristics of Bluff Bodies Using Fluidic Actuators," *AIAA* Paper 97-2004, June 1997.
4. B. Smith and A. Glezer, "The formation and evolution of synthetic jets", *Physics of Fluids*, **10**, No. 9, pp. 2281-2297, Sept. 1998.
5. M. Amitay, B.L. Smith, and A. Glezer, "Aerodynamic Flow Control Using Synthetic Jet Technology," *AIAA* Paper 98-0208, Jan. 1998.
6. R. Bryant, R. Fox, J. Lachowicz, and F. Chen, "Piezoelectric synthetic jets for aircraft control surfaces", *Proceedings of SPIE*, **3674**, pp. 220-227, 1999.
7. F.T. Calkins and D.J. Clingman, The Boeing Company, "Vibrating Surface Actuators for Active Flow Control", *Proceedings of SPIE,* **4698**, pp. 85-96, 2002.
8. M. Sugiyama, R. Oshima and F.E. Fujita, *Trans. Jpn. Inst. Met*., **27**, pp. 719, 1986
9. R.D. James and W. Wuttig, "Magnetostriction of martensite", *Phil. Mag. A,* **77**, pp.1273-1299, 1998.
10. H. Kato, T. Wada, Y. Liang, T. Tagawa, M. Taya and T. Mori, "Martensite structure in polycrystalline Fe–Pd", *Materials Science and Engineering A*, **332**, pp. 134–139, 2002.
11. T. Wada, Y. Liang, H. Kato, T. Tagawa, M. Taya and T. Mori, "Structure Change and Straining in Fe-Pd polycrystals by Magnetic Field", *Mater Sci Eng-A* , 2002*, submitted.*
12. Y. Liang, Y. Sutou, T. Wada, C. Lee, M. Taya and T. Mori, "Magnetic Field-induced Reversible Actuation Using Ferromagnetic Shape Memory Alloys", *Scripta Mat.,* 2002*,* submitted.
13. H. Kato, T. Wada, T. Tagawa, Y. Liang and M. Taya, "Development of Ferromagnetic Shape Memory Alloys Based on FePd alloy and Its Applications", *Proceedings of Mater. Sci. for 21th Centry, The Soc. of Mater. Sci. Japan,***Col. A**, pp.296-305, 2001.
14. Y. Liang, T. Wada, T. Tagawa and M. Taya, "Model Calculation of Stress-Strain Relationship of Polycrystalline Fe-Pd and 3D Phase transformation Diagram of Ferromagnetic Shape memory Alloys", *Proceedings of SPIE,* **4699**, pp. 206-216, 2002.
15. T. Wada and M. Taya, "Spring-based actuators", *Proceedings of SPIE,* **4699**, pp. 294-302, 2002,
16. K. Oguri, Y. Ochiai, Y. Nishi, S. Ohino and Y. Uchida, *Extended Abstracts of 9th Intelligent Materials Forum, Mitoh Science and Tech*, Tokyo, March 16, pp.24-25, 2000.

17 S.P. Timoshenko and J. N. Goodier, "Theory of elasticity", New York, McGraw-Hill, 1970.